

Robust constraints on past CO₂ climate forcing from the boron isotope proxy

2

Hain, M.P.^{1*}, Foster, G.L.², Chalk, T.²

4 ¹ UC Santa Cruz, Earth and Planetary Science, Santa Cruz CA 95064, USA

² University of Southampton, Ocean and Earth Sciences, SO143ZH Southampton, UK

6 * Correspondence to: mhain@ucsc.edu

8 **The atmospheric concentration of the greenhouse gas carbon dioxide, CO₂, is**
intimately coupled to the carbon chemistry of seawater, such that the radiative
10 **climate forcing from CO₂ can be changed by an array of physical, geochemical and**
biological ocean processes. For instance, biological carbon sequestration, seawater
12 **cooling and net CaCO₃ dissolution are commonly invoked as the primary drivers of**
CO₂ change that amplify the orbitally-paced ice age cycles of the late Pleistocene.
14 **Based on first-principle arguments with regard to ocean chemistry we demonstrate**
that seawater pH change (ΔpH) is the dominant control that effectively sets CO₂
16 **radiative forcing (ΔF) on orbital timescales, as is evident from independent late**
Pleistocene reconstructions of pH and CO₂. In short, all processes relevant for CO₂
18 **on orbital timescales, including temperature change, cause pH to change to bring**
about fractional CO₂ change so as to yield a linear relationship of ΔpH to CO₂
20 **climate forcing. Further, we show that ΔpH and CO₂ climate forcing can be**
reconstructed using the boron isotope pH-proxy more accurately than absolute pH
22 **or CO₂, even if seawater boron isotope composition is poorly constrained and**
without information on a second carbonate system parameter. Thus, our formalism
24 **relaxes otherwise necessary assumptions to allow the accurate determination of**
orbital timescale CO₂ radiative forcing from boron isotope-pH reconstructions
26 **alone, thereby eliminating a major limitation of current methods to estimate our**
planet's climate sensitivity from the geologic record.

28

Key points: (1) Radiative forcing by CO₂ linearly related to pH change, second carbonate system
30 parameter not required; (2) Using the boron isotope proxy, uncertainty of seawater boron isotopic
composition has weaker effect on pH change than absolute pH; (3) Short time slices of high-resolution
32 boron isotope data better suited to reconstruct climate forcing than long-term, low-resolution records

1. Introduction

34 Atmospheric carbon dioxide (CO₂) is a greenhouse gas that causes a radiative forcing of
+3.7Wm⁻² per CO₂ doubling (e.g., Myhre et al., 1998; Byrne and Goldblatt, 2014) and
36 changes in CO₂ have been identified as important drivers of climate change in the
geologic past (e.g., Zachos et al., 2008; Sigman et al., 2010; Shakun et al., 2012).
38 Reconstructing CO₂ change and its associated climate forcing from the geologic record is
important for our understanding of the history of physical, chemical and biological
40 changes in the Earth system. In particular, reconstructing the relationships between CO₂
climate forcing and climatic parameters such as temperature, ice sheet mass and sea level
42 provides valuable insights into the couplings and feedbacks operating within Earth's
climate system and their dependence on the background climate state (e.g., Martinez-Boti
44 et al., 2015; Chalk et al., 2017). In the context of ongoing warming dominated by
anthropogenic carbon emissions Earth's climate sensitivity, the average temperature
46 change per CO₂ doubling, has become a contested parameter of central importance
(IPCC, 2014). Given reconstructions of CO₂ and global temperature change it is possible
48 to estimate climate sensitivity from the geologic record (e.g., PALEOSENS Project
Members, 2012; Rohling et al., 2017), offering an important test for estimates based
50 purely on computational climate models (e.g., Andrews et al., 2012) and helping to refine
estimates of today's climate sensitivity (e.g., Knutti et al., 2017; Goodwin et al., 2018).
52 This is particularly true for past climate intervals that are warmer than the present,
implicitly integrating all known and unknown climate feedbacks operating in the Earth
54 system. However, other than for the last 800 thousand years when ice core records
accurately capture CO₂ change and its climate forcing, most methods used to reconstruct
56 CO₂ in the more distant and typically warmer-than-present geological past are indirect
and generally associated with substantial stochastic and systematic uncertainties (e.g.,
58 Royer, 2006; Hemming and Hönisch, 2007; Breecker et al., 2010; Pagani, 2014; Franks
et al., 2014; Foster and Rae, 2016). These systematic uncertainties in reconstructing
60 atmospheric CO₂ need to be overcome if we hope to robustly constrain the mechanisms
of climate change in general and climate sensitivity in particular from the geologic
62 record.

64 It is well established that pH and CO₂ are closely tied by seawater carbonate chemistry
(Figure 1), with closely aligned contours of constant pH and CO₂. We note further that
66 the spacing of contours of constant pH and log₁₀CO₂ is very similar, which suggests a
near linear relationship between H⁺ and CO₂. In this study we formally examine this
68 relationship in the context of the boron isotope pH proxy. Our main point is to greatly
relax assumptions that are currently required in the reconstruction of CO₂ radiative
70 forcing based on the boron isotope pH proxy, thereby also eliminating a significant
source of unnecessary uncertainty and facilitating the exploration of climate sensitivity
72 throughout at least the last 65 million years.

74 This manuscript is organized as follows. First, in section 2, we lay out the theory that
underpins our formalism of the relationship between pH change (ΔpH) and CO₂ radiative
76 forcing (ΔF). Then we use mathematical derivations and numerical solutions to
demonstrate the reason why ΔpH and ΔF change in unison regardless of whether these
78 changes are caused by the addition/removal of carbon and CaCO₃ or increases/decreases
in temperature. Second, in section 3, we show that the observed relationship of ΔpH
80 change and independently reconstructed ΔF from ice core measurements of the last 260
thousand years indeed agrees with our theory, that ΔpH can be robustly reconstructed
82 using the boron isotope pH proxy even if the boron isotopic composition of seawater is
poorly constrained, and that applying our formalism can yield useful constraints on
84 climate sensitivity. Finally, in section 4, we critically assess the caveats and assumptions
of our formalism, discussing specifically when our approach should not be applied and
86 considerations for the sampling strategy best suited to constrain ΔF and climate
sensitivity from the geologic record. Overall, our study suggests that it is possible to use
88 the boron isotope pH proxy to derive robust estimates of past ΔpH , ΔF and climate
sensitivity even if (a) the cause of past CO₂ change is unknown, (b) the boron isotopic
90 composition of seawater is poorly constrained, and (c) without information on a second
carbonate system parameter.

92

94 **2. Formalism and derivations**

If the goal is to estimate absolute CO₂ concentrations based on reconstructed pH then
 96 there are no shortcuts to the established formalism (e.g., Zeebe and Wolf-Gladrow,
 2001), which requires e.g. accurate measurement of boron isotopic composition of
 98 planktonic foraminifera, correction for vital effects, temperature and salinity
 reconstructions, accurate knowledge of seawater boron isotopic composition, equilibrium
 100 constant corrections for seawater major ion change, and a fully independent estimate of a
 second carbon chemistry parameter. The latter point especially is a major problem
 102 because no method currently exists to reconstruct seawater carbon concentration or
 alkalinity and their changes over geologic time. However, to calculate CO₂ climate
 104 forcing (ΔF , in Wm⁻²) we do not need to know absolute CO₂, or even absolute CO₂
 change, but only fractional CO₂ change (i.e., the change in the logarithm of CO₂,
 106 $\Delta \log \text{CO}_2$):

$$108 \quad \Delta F = \alpha_{2x\text{CO}_2} * \Delta \log_2 \text{CO}_2 = \frac{\alpha_{2x\text{CO}_2}}{\log_{10} 2} * \Delta \log_{10} \text{CO}_2 \quad (\text{eq. 1})$$

110 where $\alpha_{2x\text{CO}_2}$ is the sensitivity of the radiative balance per CO₂-doubling, $\Delta \log_2 \text{CO}_2$. For
 large parts of the subtropical and tropical ocean the carbon and acid/base chemistry of
 112 surface waters remain near equilibrium with atmospheric CO₂ because of shallow mixed
 layer depth and strong density stratification that greatly restricts exchange between
 114 equilibrating surface water and underlying waters (Takahashi et al., 2002, 2009;
 Rödenbeck et al., 2013). Assuming that surface water CO₂ partial pressure in these
 116 regions tracks atmospheric CO₂ the fractional CO₂ change relative to a reference,
 $\Delta \log_{10} \text{CO}_2 = [\log_{10} \text{CO}_2] - [\log_{10} \text{CO}_2]_{\text{reference}}$, can be expressed as follows:

118



$$120 \quad \text{CO}_2 = \frac{\text{H}^+ * \text{HCO}_3^-}{K_0 * K_1} \quad (\text{eq. 2b})$$

$$\log_{10} \text{CO}_2 = \log_{10} \text{HCO}_3^- + pK_0 + pK_1 - pH \quad (\text{eq. 2c})$$

$$122 \quad \Delta \log_{10} \text{CO}_2 = \Delta \log_{10} \text{HCO}_3^- + \Delta pK_0 + \Delta pK_1 - \Delta pH \approx -\Delta pH \quad (\text{eq. 2d})$$

124 Equation 2a is the chemical equation for the equilibrium of reversible CO₂ hydration and
deprotonation to bicarbonate and free proton, and Equation 2b quantitatively describes
126 this standard relationship between CO₂ and seawater carbonate chemistry. To yield a
distinct pH term in Equation 2c we take the logarithm of equation 2b. To write Equation
128 2d as an expression that relates fractional CO₂ change ($\Delta\log_{10}\text{CO}_2$) to pH change (ΔpH)
we take the difference between two states of carbonate chemistry written in the form of
130 Equation 2c. The other terms appearing in Equation 2 are the bicarbonate concentration
HCO₃⁻, and the carbonate chemistry equilibrium constants K₀ and K₁. Bicarbonate is by
132 far the dominant form of carbon and therefore approximates the total dissolved inorganic
carbon (DIC) concentration. The carbonate system equilibrium constants change with
134 temperature, salinity and seawater major ion composition.

136 The basic argument of this study is that the right-hand side of equation 2d is dominated
by ΔpH , and thus past fractional CO₂ change may be usefully constrained by
138 reconstructing pH change alone. If so, combining equations 1 and 2 yields a linear
relationship between pH change (ΔpH) and climate forcing from atmospheric CO₂
140 change (ΔF):

$$142 \quad \Delta F \approx 3.7 \frac{W}{m^2} * \Delta\log_2 H^+ = -12.3 \frac{W}{m^2} * \Delta\text{pH} \quad (\text{eq. 3})$$

144 Our formalism posits that fractional CO₂ change is dominantly caused by pH change,
without specifying the set of processes responsible for the pH change and without
146 assessing the magnitude of the error incurred by using that approximation. In the
following sections we demonstrate that both carbon and CaCO₃ addition/removal (section
148 2.1) as well as the temperature effects on CO₂ solubility and equilibrium constants
(section 2.2) indeed cause very similar fractional change in H⁺ and CO₂, thereby yielding
150 a linear relationship between ΔpH and ΔF as posited by our formalism.

152 **2.1 Carbon and CaCO₃ addition/removal**

The carbon chemistry of seawater is tied to the overall concentration of dissolved
154 inorganic carbon (DIC) and the relative excess of dissolved bases over acids, alkalinity

(ALK). Biological production or respiration of soft-tissue organic matter mainly removes
156 or adds carbon to seawater, with only a very small effect on ALK. Conversely, biological
production of CaCO_3 and its dissolution act to change ALK and DIC in a strict 2-to-1
158 ratio. The formalism outlined above presumes that the addition or removal of both DIC
and CaCO_3 causes most of its effect on CO_2 by changing the partitioning of DIC among
160 carbonic acid, bicarbonate ion and carbonate ion, as reflected by pH change, rather than
by changing the total dissolved carbon concentration itself (i.e., little change in the HCO_3^-
162 term in Equation 2). To assess the validity of this assertion we impose DIC and CaCO_3
addition/removal and use a carbonate chemistry solver to calculate the resulting changes
164 in pH and CO_2 (Figure 2; see panel a for DIC perturbation and panel b for CaCO_3
perturbation). Our formalism posits that the fractional change in H^+ equals the fractional
166 change in CO_2 , such that $\Delta \log_{10} \text{CO}_2$ equals ΔpH (i.e., solid black line in Figure 2d).
When cross-plotting calculated pH and CO_2 (on a logarithmic axis) we find that both DIC
168 and CaCO_3 addition/removal result in a linear pH-to- $\log_{10} \text{CO}_2$ relationship, but the slope
of that relationship is about 30% steeper for DIC and about 10% less steep for CaCO_3
170 addition/removal than posited by our formalism. That is, while our basic formalism
presumes an equal magnitude of ΔpH and $\Delta \log_{10} \text{CO}_2$ (e.g., equation 2) the consistent
172 deviations from that expectation for DIC and CaCO_3 addition/removal span an end-
member $\Delta \log_{10} \text{CO}_2 / \Delta \text{pH}$ range of about -1.3:1 and -0.9:1 that needs to be propagated
174 when using Equation 3 to infer CO_2 climate forcing from pH change.

176 To clarify why DIC and CaCO_3 addition/removal cause $\Delta \log_{10} \text{CO}_2 / \Delta \text{pH}$ that deviates
from unity and to demonstrate that these deviations are robust and expected it is useful to
178 consider the formal mathematical expressions of CO_2 change in response to a DIC
perturbation (i.e., δ_{C}) and a CaCO_3 perturbation (i.e., δ_{CaCO_3}), respectively, at constant
180 temperature and salinity (i.e., no change in the equilibrium constants; see also section 2.2
for changing equilibrium constants in response to temperature change). That is, we wish
182 to derive the partial derivatives of equilibrium CO_2 and equilibrium H^+ , which depend on
bicarbonate ion (HCO_3^-) and carbonate ion (CO_3^{2-}) concentration:

$$184 \quad \text{CO}_2 = \frac{\text{H}^+ * \text{HCO}_3^-}{K_0 * K_1} \quad (\text{eq. 4a})$$

$$H^+ = \frac{K_2 * HCO_3^-}{CO_3^{2-}} \quad (\text{eq. 4b})$$

186

In order to write the partial derivatives of CO_2 and H^+ we need to know the bicarbonate
 188 and carbonate ion partial derivatives to incremental chemical change, and we use the CPF
 (carbonate proton fraction) notation of Hain et al. (2015) to keep our expressions concise.
 190 CPF equates to the fraction of total seawater buffering that is due to the
 bicarbonate/carbonate ion buffer (i.e., seawater CPF of about -0.65 means that per unit of
 192 acid added carbonate ion is reduced and bicarbonate increased by 0.65 units):

$$\frac{\delta CO_3^{2-}}{\delta C} = CPF \approx \frac{-1}{1+B(OH)_4^-/CO_3^{2-}} \sim -0.65 \quad (\text{eq. 5a})$$

$$194 \quad \frac{\delta HCO_3^-}{\delta C} = 1 - CPF \quad (\text{eq. 5b})$$

$$\frac{\delta CO_3^{2-}}{\delta ALK} = -CPF \quad (\text{eq. 5c})$$

$$196 \quad \frac{\delta HCO_3^-}{\delta ALK} = CPF \quad (\text{eq. 5d})$$

198 The partial derivatives of H^+ and CO_2 with respect to small perturbations of DIC and
 ALK (δ_C and δ_{ALK}) are obtained using the quotient and product rule, respectively, and
 200 substituting equations 5a-d to take the place of the bicarbonate and carbonate ion partial
 derivatives:

$$202 \quad \frac{\delta_C H^+}{\delta C} = \frac{(1-CPF)*K_2}{CO_3^{2-}} - \frac{CPF*K_2*HCO_3^-}{(CO_3^{2-})^2} \quad (\text{eq. 6a})$$

$$\frac{\delta_{ALK} H^+}{\delta ALK} = \frac{(CPF)*K_2}{CO_3^{2-}} - \frac{-CPF*K_2*HCO_3^-}{(CO_3^{2-})^2} \quad (\text{eq. 6b})$$

$$204 \quad \frac{\delta_C CO_2}{\delta C} = \left\{ \frac{\delta HCO_3^-}{\delta C} * \frac{H^+}{K_0 * K_1} \right\} + \left[\frac{\delta H^+}{\delta C} * \frac{HCO_3^-}{K_0 * K_1} \right] = \left(\{1 - CPF\} + \left[1 - CPF - \frac{H^+}{K_2} CPF \right] \right) * \frac{CO_2}{HCO_3^-} \quad (\text{eq. 6c})$$

$$206 \quad \frac{\delta_{ALK} CO_2}{\delta ALK} = \left\{ \frac{\delta HCO_3^-}{\delta ALK} * \frac{H^+}{K_0 * K_1} \right\} + \left[\frac{\delta H^+}{\delta ALK} * \frac{HCO_3^-}{K_0 * K_1} \right] = \left(\{CPF\} + \left[CPF + \frac{H^+}{K_2} CPF \right] \right) * \frac{CO_2}{HCO_3^-} \quad (\text{eq. 6d})$$

208

The partial derivative of H^+ and CO_2 with respect to small perturbation of $CaCO_3$ (i.e.,
 210 δ_{CaCO_3}) is simply the sum of equations 6a/b and 6c/d weighted by the 2:1 stoichiometric
 ALK-to-DIC ratio of $CaCO_3$:

$$212 \quad \frac{\delta_{CaCO_3}H^+}{\delta_{CaCO_3}} = \frac{\delta_{CH^+}}{\delta C} + 2 * \frac{\delta_{ALK}H^+}{\delta_{ALK}} \quad (\text{eq. 7a})$$

$$\frac{\delta_{CaCO_3}CO_2}{\delta_{CaCO_3}} = \frac{\delta_{CCO_2}}{\delta C} + 2 * \frac{\delta_{ALK}CO_2}{\delta_{ALK}} \quad (\text{eq. 7b})$$

214

To arrive at the final desired expressions of fractional CO₂ change, we separate the differential and rearrange equations 6c and 7b:

$$\frac{\delta_{CCO_2}}{CO_2} = \left(\{1 - CPF\} + \left[1 - CPF - \frac{H^+}{K_2} CPF \right] \right) * \frac{\delta C}{HCO_3^-} \quad (\text{eq. 8a})$$

$$218 \quad \frac{\delta_{CaCO_3}CO_2}{CO_2} = \left(\{1 + CPF\} + \left[1 + CPF + \frac{H^+}{K_2} CPF \right] \right) * \frac{\delta_{CaCO_3}}{HCO_3^-} \quad (\text{eq. 8b})$$

220 Both equations relate left-hand side fractional CO₂ change (i.e., incremental CO₂ change
 221 δ CO₂ divided by background CO₂) to its underlying carbon chemistry causes due to
 222 carbon addition (i.e., eq. 8a: incremental carbon addition δ C divided by background
 223 bicarbonate ion concentration) and CaCO₃ addition (i.e., eq. 8b: incremental CaCO₃
 224 addition δ CaCO₃ divided by background bicarbonate ion concentration). The curly
 225 brackets on the right-hand side are arranged to highlight the effect of changing
 226 bicarbonate concentration whereas the square brackets highlight the effects of changing
 227 pH.

228

Substituting reasonable values for H⁺/K₂ and CPF into equations 8a and 8b we find that
 230 the pH effect dominates over the effect of bicarbonate abundance, in the case of DIC
 231 addition by about 3.4-fold (i.e., a square bracket pH change term of 5.55 relative to the
 232 curly bracket term of 1.65 for the effect of bicarbonate abundance, equation 8a) and in
 233 the case of CaCO₃ addition by 10-fold (i.e., a square bracket pH change term of -3.55
 234 relative to the curly bracket term of 0.35, equation 8b). That is, the relationships between
 Δ pH and $\Delta \log_{10}$ CO₂ are not exactly -1:1 as approximated in equation 2d, but based on
 236 equation 8 we estimate -1:1.3 for carbon addition/removal and -1:0.9 for CaCO₃
 237 addition/removal (the range between these end-members is shown as gray shading in
 238 Figure 2d).

240 The slightly stronger and weaker than predicted CO₂-to-pH relationships for incremental
DIC and CaCO₃ addition/removal, respectively, are quantitatively consistent with the
242 carbonate chemistry solver results shown in Figure 2, underscoring on a mechanistic
level that pH change caused by DIC and CaCO₃ addition/removal is the dominant driver
244 of CO₂ change whereas the much weaker effect of changing bicarbonate abundance is
responsible for the deviation of the ΔpH -to- $\Delta\log_{10}\text{CO}_2$ relationship from the -1:1 solely
246 pH-driven slope (i.e., solid black line in Figure 2d). Based on these deviations, if pH
change is known exactly then $\Delta\log_{10}\text{CO}_2$ and CO₂ climate forcing can be estimated to
248 within the end-member bounds of -10% for purely CaCO₃-caused and +30% for purely
DIC-caused carbon chemistry change (i.e., gray shading in Fig 1d), with any combination
250 of these drivers yielding less bias relative to the formalism of equations 2 and 3. Later in
the manuscript, in section 3.3, we will use this theoretically derived end-member
252 uncertainty envelope when estimating CO₂ climate forcing from pH change.

254 **2.2 Temperature change**

All of what is said above ignores the strong effects of temperature on the solubility of
256 CO₂ in seawater and on the equilibrium constants that govern the deprotonation equilibria
of carbonic acid and bicarbonate ion: i.e., K_0 , K_1 and K_2 . This raises the question if
258 temperature change associated with CO₂ climate forcing can reduce the utility of our
formalism for estimating CO₂ climate forcing from reconstructed pH change. That is,
260 does temperature change CO₂ independently of pH? To address this question we derive
the sensitivity of fractional CO₂ change to incremental change in temperature, and we use
262 a carbonate chemistry solver to confirm that temperature change cause fractional CO₂ and
H⁺ changes very close to the posited -1:1 relationship.

264

Analogous with the derivation of the DIC and CaCO₃ effects above, we use the product
266 rule to arrive at the partial derivative of H⁺ and CO₂, but this time due to temperature
change in absence of DIC or ALK perturbation. Since the speciation of the set
268 concentration of carbon is constrained by the set ALK we take the partial derivatives of
bicarbonate and carbonate ion to be zero (a very good approximation) and only consider

270 changes in the equilibrium constants and the minor species $[H^+]$ and (implicitly) carbonic
acid:

$$272 \quad \frac{\delta_T H^+}{\delta T} \cong \frac{HCO_3^-}{CO_3^{2-}} * \frac{\delta_T K_2}{\delta T} = \frac{CO_2}{K_2} * \frac{\delta_T K_2}{\delta T} \quad (\text{eq. 9a})$$

$$\frac{\delta_T CO_2}{\delta T} \cong \left\{ \frac{-CO_2}{K_0 * K_1} * \frac{\delta_T (K_0 * K_1)}{\delta T} \right\} + \left[\frac{CO_2}{K_2} * \frac{\delta_T K_2}{\delta T} \right] \quad (\text{eq. 9b})$$

274

To arrive at the final desired expression of fractional CO_2 change in response to
276 temperature change we separate the differential and rearrange equation 9b:

$$\frac{\delta_T CO_2}{CO_2} \cong \left\{ -\frac{\delta_T K_0}{K_0} - \frac{\delta_T K_1}{K_1} \right\} + \left[\frac{\delta_T K_2}{K_2} \right] \approx \left(\left\{ \frac{3\%}{^\circ C} - \frac{2.5\%}{^\circ C} \right\} + \left[\frac{3.5\%}{^\circ C} \right] \right) * \delta T \quad (\text{eq. 10})$$

278

280 From this approximation we find three dominant terms governing CO_2 sensitivity to
incremental warming that can be described as: (K_0 term) a fractional decrease in CO_2
282 solubility K_0 causes a fractional CO_2 increase; (K_1 term) at a given pH a fractional
increase in the bicarbonate-to-carbonic acid equilibrium constant K_1 causes a fractional
284 CO_2 decrease; and (K_2 term) constant DIC and ALK demand that the carbonate-to-
bicarbonate ion ratio is nearly constant so that a fractional increase in the carbonate-to-
286 bicarbonate ion equilibrium constant K_2 causes a fractional increase of H^+ . This latter
fractional H^+ increase, a pH decline, translates to a fractional increase in CO_2 . Put a
288 different way, the K_0 and K_1 effects (curly bracket in equation 10) operate mainly by
changing the abundance and solubility of the least abundant dissolved inorganic carbon
290 species, carbonic acid, whereas the K_2 effect (square bracket) changes the pH at which
the main seawater acid/base buffer, bicarbonate-to-carbonate ion, is at equilibrium.

292

When using a carbonate chemistry solver we find the net sensitivity of CO_2 to
294 temperature change (at constant DIC and ALK) is about a 4% increase per degree of
warming (Figure 2c), which agrees very well with the sum of the three individual effects
296 isolated in equation 10. Likewise, the carbonate chemistry solver yields about 3.5% H^+
increase per degree of warming, fully consistent with the square bracket K_2 term in
298 equation 10. All three terms in equation 10 have a similar magnitude, but the two terms
(K_0 , K_1) that operate through carbonic acid have opposite sign and nearly cancel each

300 other whereas the K_2 term that operates through pH is unopposed. For this reason, the
pH-driven CO_2 change (square bracket) is 7-fold greater than the CO_2 change driven by
302 the combination of carbonic acid solubility and deprotonation (curly bracket; equation
10). Thus, by fortuitous coincidence, the sensitivities of fractional H^+ change and
304 fractional CO_2 change to incremental warming or cooling is approximately the same
(Figure 2c), yielding a -1:1.14 ΔpH -to- $\Delta\log_{10}\text{CO}_2$ relationship that is close to the -1:1
306 approximation in equation 2d, and it falls within the end-member range of DIC and
 CaCO_3 addition/removal (see section 2.1). That is to say, the net effect of temperature on
308 fractional CO_2 change can be estimated from pH change in the very same way as CO_2
change caused by the addition or removal of DIC and CaCO_3 (Figure 2c and 2d).

310

3 Validation and Applications

312 3.1 Relationship of pH and ice core CO_2

Our formalism, equation 3, suggests that on orbital timescales there should be a linear
314 relationship between CO_2 radiative climate forcing and pH change of the well-
equilibrated subtropical ocean surface, with the slope of that relationship effectively set
316 by the independently determined (e.g., Myhre et al., 1998; Byrne and Goldblatt, 2014)
radiative effect per CO_2 doubling. We test this assertion by combining the continuous late
318 Pleistocene ice core atmospheric CO_2 record with overlapping boron isotope
measurements on planktonic foraminifera. Recently collected data from ODP Site 999
320 (Chalk et al., 2017) offers the unique opportunity to rigorously test the theory over the
last 260 thousand years.

322

Ice core CO_2 data are precise, accurate (e.g., Bereiter et al., 2015) and using equation 1
324 can be easily converted into climate forcing, ΔF . Foraminiferal boron isotope data can be
used to reconstruct surface pH given auxiliary knowledge of temperature and bulk
326 seawater boron isotopic composition (Vengosh et al., 1991; Hemming and Hanson, 1992;
Spivack et al., 1993; Zeebe and Wolf-Gladrow, 2001; Foster and Rae, 2016). For the
328 purpose of this proof-of-concept test we use Mg/Ca-based SST data only to account for
the temperature effect on the pH reconstruction (i.e., pK_B temperature dependence; using
330 our formalism we need not calculate the carbonate chemistry equilibrium constants pK_0 ,

pK₁ and pK₂) and we presume known modern boron isotopic composition of seawater
332 (39.61 ‰; Foster et al., 2010), as is appropriate for the late Pleistocene given the multi-
million year ocean residence time of boron (Spivack and Edmont, 1987; Lemarchand et
334 al., 2002). The new boron isotope and Mg/Ca data (Chalk et al., 2017) that overlaps with
the ice core CO₂ record was measured at the University of Southampton using established
336 and extensively documented methods (Foster, 2008; Foster et al., 2013). The 1σ age
uncertainty of the data is 1 kyrs and 1.5 kyrs for the for data points younger and older
338 than 10 kyrs, respectively.

340 To account for the significant age uncertainty of the boron isotope data when compared
to the well-dated ice core data we calculate the cumulative probability density of the ice
342 core data within the ±4σ age uncertainty interval, normalized by their respective
likelihood given the age difference. This approach yields small uncertainty in CO₂-driven
344 ΔF at times that coincide with intervals of the ice core record with relatively constant
CO₂, and it yields large ΔF uncertainty for ages corresponding to rapid CO₂ change. That
346 is, while the ice core CO₂ data itself is very accurate and well-dated the age uncertainty
of the boron isotope data implies significant uncertainty in ΔF_{ice-core} at the time of the
348 δ¹¹B-based reconstruction of pH. Plotting ΔF_{ice-core} as a function of the corresponding
reconstructed pH yields a strong apparent negative correlation (Figure 3). We also plot
350 the 1σ uncertainty intervals corresponding to the internal reproducibility of the
underlying boron isotope measurement (horizontal error bars) as well as the 1σ of ΔF_{ice-}
352 core corresponding to the age uncertainty the sediment samples (vertical error bars), which
together can explain most of data scatter.

354
To determine the best-fitting linear model we use York regression (York et al., 2004),
356 which accounts for uncertainty in both x and y. The dark and light blue shading in Figure
3 represents the 1σ and 2σ envelope of the maximum likelihood model (i.e., ΔF/ΔpH = -
358 13.3 W/m²; with 1σ of 0.5 W/m²). That is, the best-fitting model through the data is very
close to the theoretical ΔF/ΔpH relationship of -12.3 W/m² (solid black line in Figure 3)
360 and indeed we cannot reject the null hypothesis that the data results from a strict
adherence to our basic formalism (i.e., equation 3) plus random Gaussian error. This error

362 term can be estimated from the residuals to be 1σ of $\sim 0.32\text{W/m}^2$ and it corresponds to the
superposition of boron isotope measurement uncertainty, age error, air/sea
364 disequilibrium, etc.

366 In the above analysis we have validated our basic formalism without considering that
equation 3 is a useful approximation rather than a first-principle law. As is evident from
368 Figure 2d and equations 8 and 10 the first principle slope of the $\Delta F/\Delta\text{pH}$ relationship is
 $\sim 14\text{-}30\%$ steeper if the driving process is a change in temperature or DIC
370 addition/removal, while it is $\sim 10\%$ less steep when caused by CaCO_3 addition/removal.
In this context, we can reject the null hypothesis that overall glacial-interglacial CO_2
372 change and its climate forcing were exclusively driven by either biological sequestration
of carbon or ocean alkalinity changes via the open system CaCO_3 cycle. This outcome is
374 consistent with the large body of evidence that glacial cooling, carbon sequestration from
the atmosphere and upper ocean via the biological pump into the deep ocean, as well as
376 whole ocean alkalinity increase related to transient and steady state lysocline change all
contributed to ice age CO_2 drawdown (e.g., Sigman and Boyle, 2000; Martinez-Garcia,
378 2014; Sigman et al., 2010; Hain et al., 2014; Wang et al., 2017). Because the best-fitting
regressed slope falls between the CaCO_3 end-member on one side and the temperature
380 and DIC end-members on the other side we conclude that a relatively large portion of
overall glacial/interglacial CO_2 change appears to have been driven by changes in whole
382 ocean alkalinity related to transient imbalances in the ocean's open system CaCO_3 cycle,
resonating with one of the earliest hypothesis to explain these changes (Broecker and
384 Peng, 1987). All of these processes have acted at different times in the glacial progression
(e.g., Hain et al. 2010), such that their relative contribution to CO_2 drawdown and the
386 effective relationship between CO_2 and pH evolved with time. In this context, it seems
plausible to decompose the relative contribution of DIC, alkalinity and temperature
388 changes to overall glacial/interglacial CO_2 change based on the regression of $\Delta F/\Delta\text{pH}$,
but such analysis would require additional global carbon cycle modeling that is beyond
390 the scope of this study. For the purpose of this work we note that the empirical $\Delta\text{pH}/\Delta F$
slope falls well within the end member $\Delta\text{pH}/\Delta F$ range for DIC and CaCO_3 changes, and
392 that this range can be used to represent the uncertainty in the conversion from ΔpH to ΔF .

394 **4.2 Seawater boron isotope composition**

The approach described above only requires a record of past pH changes to reconstruct
396 CO₂ climate forcing, thereby making independent knowledge of background ocean
carbon concentration (DIC) and temperature for the purpose of calculating the carbon
398 chemistry equilibrium constants K₀, K₁ and K₂, unnecessary. However, to reconstruct pH
from boron isotope data (i.e., δ¹¹B_{borate}) still requires independent constraints on the bulk
400 boron isotopic composition of seawater (δ¹¹B_{SW}) as well as temperature and salinity for
the purpose of calculating the borate/boric acid equilibrium constant pK_B (e.g., Zeebe and
402 Wolf-Gladrow, 2001), which is weakly dependent also on seawater major ion
composition (Hain et al, 2015) and may thus require minor correction for the deep
404 geologic past (Henehan et al., 2016). This raises the question: Can we use boron isotope
data to reconstruct CO₂ climate forcing in deep geologic time, when bulk seawater boron
406 isotopic composition is poorly constrained and temperature reconstructions are
questionable at least in their absolute sense? Or, put a different way, is the boron isotope
408 pH proxy inherently more robust in reconstructing past pH *change* than in reconstructing
absolute pH? To answer these questions we first consider the established boron isotope
410 pH proxy equation for a single sample (Zeebe and Wolf-Gladrow, 2001):

412
$$pH_0 = pK_B - \log_{10} \left(\frac{\delta_0 - \delta_{SW}}{\delta_{SW} - \alpha * \delta_0 - \epsilon} \right) \quad (\text{eq. 11})$$

414 where ε and α are the equilibrium boron isotope effect and fractionation factor (i.e.,
27.2‰ and 1.0272; see Klochko et al., 2006), δ_{SW} is the boron isotopic composition of
416 bulk seawater, δ₀ is the reconstructed boron isotopic composition of borate from which
pH is to be calculated, and pK_B is the borate/boric acid equilibrium constant when δ₀ was
418 formed. Accurate reconstruction of absolute pH using this formulation requires accurate
reconstruction of both δ₀ and δ_{SW}, and accurate auxiliary information on absolute
420 temperature, salinity and seawater major ion composition to calculate pK_B. Notably, δ₀
and δ_{SW} carry equivalent weight in the established boron isotope pH proxy equation but
422 for much of Earth history δ_{SW} is much more uncertain than reconstructions of δ₀.

424 To contrast the established formulation we write the proxy equation for pH change (ΔpH)
reconstructed from a set of two borate boron isotope reconstructions, δ_0 and δ_1 :

$$\begin{aligned} 426 \quad \Delta\text{pH} &= \text{pH}_1 - \text{pH}_0 = \Delta\text{pK}_B - \log_{10} \left(\frac{\delta_1 - \delta^{11}\text{B}_{\text{SW}}}{\delta_{\text{SW}} - \alpha * \delta_1 - \epsilon} * \frac{\delta_{\text{SW}} - \alpha * \delta_0 - \epsilon}{\delta_0 - \delta_{\text{SW}}} \right) \\ &= \Delta\text{pK}_B - \log_{10} \left(1 + \frac{\delta_1 - \delta_0}{\delta_{\text{SW}} - \alpha * \delta_1 - \epsilon} * \frac{(\alpha - 1) * \delta_{\text{SW}} - \epsilon}{\delta_0 - \delta_{\text{SW}}} \right) \end{aligned} \quad (\text{eq. 12})$$

428

While δ_{SW} is still required to calculate ΔpH the dominant boron isotope term in the ΔpH
430 equation is the difference between δ_1 and δ_0 , which has two very significant implications.
First, any error in δ_{SW} causes greater error in reconstructed pH than in ΔpH , such that
432 ΔpH can be more accurately reconstructed than absolute pH in the face of δ_{SW}
uncertainty. Second, the reconstructed values of δ_0 and δ_1 need to be precise but not
434 necessarily accurate as long as they carry the same systematic bias (e.g., from vital
effects, matrix differences between the sample material and the measurement standard,
436 etc.), which makes the reconstruction of ΔpH inherently more robust than the
reconstruction of absolute pH. Additionally, ΔpK_B only weakly depends on only relative
438 changes in temperature, salinity and seawater major ion composition, not absolute values,
such that ΔpK_B is smaller and can be more accurately reconstructed than pK_B . Overall,
440 our examination of the pH and ΔpH proxy equations demonstrates that reconstructions of
 ΔpH are both more accurate in the face of δ_{SW} uncertainty and more robust in the face of
442 a number of potential biases than is the reconstruction of absolute pH. We anticipate that
this finding will not come as a major surprise to practitioners in the field of boron isotope
444 geochemistry, but to our knowledge this is the first formal statement of the fact.

446 Based on the above theoretical considerations we should be able to recover the correct
relationship between CO_2 climate forcing (ΔF) and pH change (ΔpH) even if we were to
448 completely ignore temperature change (e.g., because ΔpK_B is only a relatively weak
function of temperature change) and even if we were to deliberately introduce significant
450 error in the bulk seawater boron isotopic composition (e.g., because δ_{SW} has little weight
on the value of the logarithmic term in equation 12). To demonstrate the pervasive
452 differences in the reconstruction of pH and ΔpH we turn again to the comparison of the

boron isotope measurements from ODP Site 999 and the coeval ice core record of
454 atmospheric CO₂ (as in Figure 3) but this time systematically changing the bulk seawater
boron isotopic composition ($\delta^{11}\text{B}_{\text{SW}}$, same as abbreviated δ_{SW} notation in equations 11
456 and 12) used in the calculation by $\pm 4.2\%$ around its true value of 39.61‰ (Figure 4).
Also, we find no noticeable difference when including or excluding the effect of
458 reconstructed local temperature changes on pK_{B} , and for the purpose of highlighting the
role of δ_{SW} uncertainty we show the results where pK_{B} is taken to be constant.

460

As expected the very large range of deliberately introduced offset in seawater boron
462 isotopic composition systematically increases/decreases the mean absolute pH by more
than 0.07 pH units per ‰ of $\delta^{11}\text{B}_{\text{SW}}$ change (Figure 4a). That is, absolute pH is highly
464 sensitive to the assumed $\delta^{11}\text{B}_{\text{SW}}$ (see also Pagani et al., 2005). In stark contrast, however,
the pH range covered by the ODP Site 999 dataset changes much less as $\delta^{11}\text{B}_{\text{SW}}$ is
466 manipulated, such that the regressed $\Delta F/\Delta\text{pH}$ slope changes only mildly even in the face
of substantial introduced $\delta^{11}\text{B}_{\text{SW}}$ error. Specifically, comparison of the regressed slope
468 (blue envelope) to the relationship theoretically predicted by equation 3 suggests that the
theory is a reasonably good predictor for the true ice core-derived ΔF even in the face of
470 $\delta^{11}\text{B}_{\text{SW}}$ error as large as $\pm 2\%$ (x-axis in Figure 4b), which compares favorably with the
uncertainty of $\delta^{11}\text{B}_{\text{SW}}$ reported in available reconstructions (e.g., Lemarchand et al., 2000;
472 Raitzsch and Hönisch, 2013; Greenop et al., 2017).

474 We note that we calculate the results shown in Figure 4 using the established pH proxy
equation, and that our formulation of ΔpH (i.e., equation 12) simply expresses the
476 difference between two standard pH reconstructions. The main point we intend to
demonstrate in this section is that $\delta^{11}\text{B}_{\text{SW}}$ uncertainty affects pH significantly more than it
478 does ΔpH , both reconstructed using the same established boron isotope proxy equation.
That is, the boron isotope proxy system inherently yields more robust estimates of past
480 pH change than absolute pH. Earlier we showed in theory (see section 2) and
observations (see section 3.1) that pH change (ΔpH) is a strong predictor for CO₂ climate

482 forcing. In that context, our ability to obtain robust reconstructions of ΔpH from the
boron isotope proxy is critical.

484

3.5 Climate sensitivity

486 Reconstructing CO_2 radiative forcing using the boron isotope pH proxy offers important
insights into the role of the global carbon cycle in causing climate change of the geologic
488 past. However, in the context of ongoing anthropogenic climate change and when
comparing different periods of geologic time the quantity of interest is often the climate
490 sensitivity S , which is the ratio of temperature change (ΔT) per radiative climate forcing
(ΔF) (e.g., Knutti and Hegerl, 2008):

492

$$S = \Delta T / \Delta F \quad (\text{eq. 13})$$

494

In the case that only the component of total forcing that is due to CO_2 is explicitly
496 considered the climate sensitivity calculated in this way is commonly referred to as Earth
System Sensitivity (ESS; Lunt et al. 2010), which implicitly includes climate system
498 feedbacks that are ‘fast’ (e.g., water vapor, clouds) and ‘slow’ (e.g., dust, ice sheets).
Also, there exists a spectrum of alternate definitions of climate sensitivity that explicitly
500 include the component climate forcing of a number of these “slow” processes (e.g.,
PALEOSENS, 2012; von der Heydt et al., 2016). We note that all formulations of climate
502 sensitivity require constraints on CO_2 climate forcing, which is the focus of our study, but
detailed treatment of different types and ways to calculate climate sensitivity is beyond
504 our scope here. That said, given the uncertainties of boron isotope measurements and the
range in the ΔpH -to- ΔF conversion for different end-member causes of pH change (i.e.,
506 CaCO_3 , temperature and DIC change as described above, Figure 2), we need to address
the question if our formalism can yield sufficiently accurate and precise constraints on
508 $\Delta T/\Delta F$. To address this question we need a target estimate of “true” $\Delta T/\Delta F$ and compare
it to the equivalent result based on boron isotope data. For this test we again turn to the
510 ice core CO_2 record (as compiled by Bereiter et al., 2015) to yield “true” CO_2 radiative
forcing, which we pair with two independent reconstructions of temperature change over
512 the late Pleistocene glacial/interglacial cycles (global mean surface air temperature MAT

and sea surface temperature SST taken from Martinez-Boti et al., 2015). We note that
514 SST does not reflect global mean surface temperature such that using this record is not
intended to yield bona fide estimates of climate sensitivity but to evaluate the accuracy
516 and precision of our formalism in constraining climate sensitivity. Conversely, MAT is
based on inverse model results of northern hemisphere temperature (i.e., van de Wal et
518 al., 2011) scaled to reflect global mean surface temperature for the purpose of calculating
climate sensitivity (see Martinez-Boti et al., 2015).

520

We interpolate the temperature records at the ages of the 1011 discrete ice core CO₂ data
522 points of the last 260 kyrs and determine $\Delta T/\Delta F$ by regressing the slope of temperature
change per ice core CO₂-derived climate forcing using the York regression method (York
524 et al., 2004), assuming 1σ uncertainty of 1°C and 5 ppmV for temperature and ice core
CO₂, respectively. This approach yields slopes $\Delta T_{\text{MAT}}/\Delta F_{\text{ice1011}}$ of 2.5°C/(Wm⁻²) and
526 $\Delta T_{\text{SST}}/\Delta F_{\text{ice1011}}$ of 1.2°C/(Wm⁻²), both with a 2σ regression slope uncertainty
 $\pm 0.09^\circ\text{C}/(\text{Wm}^{-2})$ (shown as shading in lower panel of Figure 5). That analysis, however,
528 is not representative of $\Delta T/\Delta F$ of the last 260 kyr (for which we have boron isotope data)
because uneven sampling results in almost half of the ice core derived CO₂ data points
530 from the last 20 kyrs, and more than 80% from the last 100kyr. When we repeat the
analysis but only include the ice core data that are closest to the ages of the boron isotope
532 record (i.e., 59 samples with ~4 kyr sample interval) we regress $\Delta T_{\text{MAT}}/\Delta F_{\text{ice59}}$ of
2.5°C/(Wm⁻²) and $\Delta T_{\text{SST}}/\Delta F_{\text{ice59}}$ of 1.3°C/(Wm⁻²), both with 2σ regression slope
534 uncertainty of $\pm 0.4^\circ\text{C}/(\text{Wm}^{-2})$ (Figure 5; MAT and SST regressions shown in red and
blue, respectively). We take these ice core CO₂-based numbers to be the “true” answer in
536 our test of the boron isotope-based reconstruction. We note that both $\Delta T_{\text{MAT}}/\Delta F_{\text{ice1011}}$ and
 $\Delta T_{\text{MAT}}/\Delta F_{\text{ice59}}$ are consistent with previous estimates of late Pleistocene ESS climate
538 sensitivity to CO₂ forcing (e.g., see $S_{[\text{CO}_2]}$ in Table 2 of PALEOSENS, 2012).

540 In determining the 2σ range of ΔF_{boron} we use the 2σ uncertainties of the boron isotope
measurement of every data point conflated with the lowest and highest end-member slope
542 of the ΔpH -to- ΔF relationship (i.e., the slope for CaCO₃ and DIC change, respectively;
see Figure 2). That is, ΔF_{boron} includes the uncertainty both of the boron isotope

544 measurement as well as the uncertainty of the conversion from ΔpH to ΔF . This treatment
makes the assumption that the ΔpH -to- ΔF slope uncertainty is independent between data
546 points, which can be justified because the reconstructed pH change of each sample is
caused by a different combination of CaCO_3 , temperature and DIC change. For the
548 temperature data to be compared with ΔF_{boron} we conflate the uncertainty of the
temperature reconstruction (1σ of $\pm 1^\circ\text{C}$, as above) with the age uncertainty of the boron
550 isotope data, yielding an effective temperature uncertainty only marginally larger than 1σ
of $\pm 1^\circ\text{C}$. The regression based on the boron isotope data yields $T_{\text{MAT}}/\Delta F_{\text{boron}}$ of
552 $2.6^\circ\text{C}/(\text{Wm}^{-2})$ with 2σ regression slope uncertainty of $\pm 0.5^\circ\text{C}/(\text{Wm}^{-2})$ and $\Delta T_{\text{SST}}/\Delta F_{\text{boron}}$
of $1.3^\circ\text{C}/(\text{Wm}^{-2})$ with 2σ of $\pm 0.4^\circ\text{C}/(\text{Wm}^{-2})$ (shown in black in Figure 5).

554

Direct measurement of CO_2 on air trapped in ice cores yields inherently much more
556 precise and accurate estimates of CO_2 climate forcing than indirect proxy-based
approaches, such as the conventional application or our new formalism for the boron
558 isotope system. Our test case illustrates that ice core-based reconstruction of $\Delta T/\Delta F$
yields more accurate and precise constraints than can be achieved based on boron isotope
560 data, but the difference is rather modest because fractional uncertainty in temperature
reconstructions is typically larger than the fractional uncertainty of the CO_2 climate
562 forcing reconstructed based on either ice core or boron isotope data and thus dominates
the uncertainty of the regressed slope $\Delta T/\Delta F$ (i.e., fractional uncertainty referring to the
564 ratio of uncertainty to the overall recorded signal). That is, our test suggests that boron
isotope data can in principle be used to reconstruct climate sensitivity with an uncertainty
566 not substantially larger than based on ice core CO_2 data, when the number of data points
is the same. More precise constraints on temperature change and more discrete data
568 points are best suited to reduce the uncertainty of the regressed climate sensitivity, rather
than further reducing the uncertainty in reconstructed CO_2 climate forcing. We highlight
570 that our formalism yields adequate constraints on climate forcing without requiring any
assumption of a second carbonate system parameter, without knowledge of the carbonate
572 chemistry equilibrium constants (i.e., pK_0 , pK_1 , pK_2 ; which are strongly dependent on
temperature and the major ion composition of seawater), and without highly precise
574 knowledge of the boron isotopic composition of seawater ($\delta^{11}\text{B}_{\text{SW}}$). Contrary to the

conventional application of the boron isotope system, our formalism yields adequate
576 constraints on climate sensitivity using only the boron isotope data, reconstructed local
temperature change (to calculate ΔpK_B for the ΔpH reconstruction, which is a weak
578 function of relative temperature change), and best guess $\delta^{11}B_{SW}$ (see section 3.4; Figure
4), all of which can be obtained from the geologic record significantly older than the
580 reach of ice cores.

582 **4 Discussion and caveats**

The boron isotope pH proxy is firmly established as a tool to reconstruct past ocean pH
584 (e.g., Zeebe and Wolf-Gladrow, 2001; Hemming and Hönisch, 2007; Rae et al., 2011;
Foster and Rae, 2016) and its usage to place constraints on past ocean acid/base
586 chemistry is rapidly increasing. Furthermore, if the sample material originates from the
highly stratified and close to air/sea equilibrated subtropical surface, with auxiliary
588 constraints on ambient temperature and an assumption on a second carbonate system
parameter (such as DIC, alkalinity, etc.) the boron isotope pH proxy is routinely extended
590 to reconstruct past atmospheric CO_2 and its radiative forcing of climate change. It is well
established (e.g., Pearson and Palmer, 2000; Raitzsch and Hönisch, 2013; Greenop et al.,
592 2017) that this conventional approach relies heavily on accurate and independent
knowledge of past seawater boron isotopic composition ($\delta^{11}B_{SW}$) and on the (explicitly or
594 implicitly) assumed seawater carbon content (DIC), alkalinity (ALK), or $CaCO_3$
saturation state. Beyond the last few million years of Earth history both $\delta^{11}B_{SW}$ and these
596 second carbonate system parameters are poorly known, thereby stifling the use of the
boron isotope proxy system to investigate the role of the global carbon cycle in forcing
598 climate change throughout most of geologic time. With this paper we hope to lay the
groundwork for the robust application of the boron isotope proxy system for geologic
600 periods when $\delta^{11}B_{SW}$, a second carbonate system parameter such as DIC, and/or absolute
temperature cannot be determined with the previously required degree of accuracy.

602

In this study we propose three main new concepts to extend the utility of the boron
604 isotope proxy system, respectively relating to (1) $\delta^{11}B_{SW}$, (2) the need for a second

carbonate system parameter, and (3) the role of temperature change via its effect on
606 carbonate chemistry equilibrium constants and Henry's law.

608 First, we demonstrate that when $\delta^{11}\text{B}_{\text{SW}}$ is poorly constrained the boron isotope proxy
system can be used to robustly reconstruct ΔpH , but not absolute pH (Fig 3). This result
610 is firmly based in first principle theory. We caution, however, that this approach is only
applicable to boron isotope time series that cover no more than a few million years
612 because it assumes that $\delta^{11}\text{B}_{\text{SW}}$ is constant within the dataset. This timescale is
fundamentally set by the ocean residence time of boron, which is canonically assumed to
614 be 10-20 million years (Lemarchand et al., 2002) but may be somewhat shorter (Greenop
et al., 2017).

616

Second, we demonstrate that that CO_2 climate forcing (ΔF) and its causal fractional CO_2
618 change ($\Delta\log\text{CO}_2$) are tightly related to pH change (ΔpH) and fractional change in
bicarbonate and DIC (i.e., $\Delta\log\text{HCO}_3^-$, $\Delta\log\text{DIC}$). We argue that both $\Delta\log\text{HCO}_3^-$ and
620 $\Delta\log\text{DIC}$ must be relatively small on timescales shorter than the oceans residence time of
carbon with respect to the geologic CO_2 sources and silicate weathering (very roughly 1
622 million years), such that ΔpH is the overwhelmingly dominant driver of atmospheric CO_2
change and its climate forcing on orbital timescales. That is, even at times when absolute
624 DIC is unknown we argue it is fair to assume that $\Delta\log\text{DIC}$ and $\Delta\log\text{HCO}_3^-$ are small
compared to ΔpH reconstructed from a boron isotope dataset that spans no more than a
626 few orbital cycles, akin to the late Pleistocene ice age CO_2 cycles that we use to validate
our formalism. We caution that relaxing the DIC constraint in this way does not apply to
628 events of abrupt carbon addition in secular steady state with carbonate compensation (i.e.,
the Paleocene-Eocene thermal maximum), in which case $\Delta\log\text{DIC}$ could significantly
630 contribute to ΔF and relying on ΔpH alone would underestimate ΔF .

632 Third, while temperature significantly affects both the conventional boron isotope pH
proxy and the partitioning of carbon between the atmosphere and seawater we show that
634 it has a surprisingly weak effect on the relationship between the range of boron isotope
measurements in a given dataset, the ΔpH reconstructed from this data, and on the

636 climate forcing ΔF inferred from it. To be clear, any information on temperature change
will improve reconstructed ΔpH and ΔF because it constrains the presumably small ΔpK
638 terms in equations 2 and 12. To achieve these improvements requires only accurate
information on temperature differentials (i.e., temperature information needs to be precise
640 but can be inaccurate) such that accurate information on absolute temperatures is not
required. This insight is very convenient even if it is the completely coincidental result of
642 the approximately linear temperature dependence of the pK equilibrium constants (i.e.,
the exponential temperature dependence of the equilibrium constants K ; $pK = -\log K$).

644

Considering the advantages and caveats outlined above, how can our new approach be
646 used to make useful inferences about past CO_2 climate forcing? And, what type of boron
isotope sampling strategy is best suited to recover robust reconstructions of CO_2 climate
648 forcing? To illustrate and discuss these questions we apply our formalism to four boron
isotope datasets (Figure 6): the orbitally-resolved record of the intensification of northern
650 hemispheric glaciation at the Plio-Pleistocene transition by Martinez-Boti et al. (2015),
the record across the Middle Miocene Climatic Optimum (MMCO) by Greenop et al.
652 (2014) that exhibits, but does not fully resolve, orbital-timescale boron isotope changes,
and the new highly-resolved late and mid Pleistocene records from ODP Site 999 (Chalk
654 et al., 2017), the former of which we used to validate our formalism.

656 All these records are short relative to the residence time of boron in the ocean, which
precludes significant change in $\delta^{11}B_{SW}$ over the duration of each time slice. Thus, we use
658 modern $\delta^{11}B_{SW}$ for the Plio-Pleistocene data (39.61‰; Foster et al., 2010), and a lower
 $\delta^{11}B_{SW}$ value of 37.82‰ for the mid-Miocene (Foster et al. 2012, Greenop et al., 2014).
660 As we demonstrate here (e.g., Figure 4), using slightly different estimates for low mid-
Miocene $\delta^{11}B_{SW}$ (e.g., Lemarchand 2002; Raitzsch and Hönisch, 2013; Greenop et al.,
662 2017) would make no significant difference because pH change reconstruction is much
less sensitive to the $\delta^{11}B_{SW}$ value than is the reconstruction of absolute pH . For all
664 datasets we calculate ΔpH relative to the average $\delta^{11}B_{borate}$ and relative to the average
reconstructed temperature of the respective dataset, using equation 12 without
666 approximation. Hence, we can plot the data on the same axes of pH change and CO_2

climate forcing, but this axis only applies to changes within each respective dataset and
668 not to changes between them.

670 The residence time of carbon relative to total weathering is about 200 thousand years but
only a fraction of total weathering is due to silicate weathering, such that fractional
672 change of ocean DIC can be assumed to be small on a roughly million-year timescale and
shorter. Hence, we cannot quantify a likely small contribution of DIC change (i.e.,
674 $\Delta \log \text{HCO}_3^-$) to climate forcing e.g., at the onset of the MMCO at 17.2-16.5 Myr or across
the duration of the Plio-Pleistocene time slice at 3.3-2.3 Myr. However, the orbital-
676 timescale changes evident in all three datasets, as well as the abrupt ~ 2.8 Myr step-
change associated with the intensification of northern hemisphere glaciation, are too rapid
678 to allow for significant DIC change and must therefore satisfy our formalism, as is
supported by the good agreement with the ice-core CO_2 data (Figure 3, Figure 6). As a
680 caution, the orbital-timescale fluctuations during the MMCO are not fully resolved, often
supported only by single low- $\delta^{11}\text{B}$ data points and thus prone to be questioned as being
682 outliers. In this context, using a boron isotope record that is sufficiently resolved to
support orbital-timescale $\delta^{11}\text{B}_{\text{borate}}$ fluctuations with multiple data points is prudent when
684 aiming to reconstruct climate forcing.

686 Based on these considerations we argue that datasets that fully resolve orbital timescales
over the course of time slices not significantly longer than about one million years are
688 most suited for the reconstruction of pH change and CO_2 climate forcing. To the best of
our knowledge such datasets are exceedingly rare at the moment, with most efforts
690 currently aimed at generating long-term, low-resolution records that require highly
uncertain corrections for $\delta^{11}\text{B}_{\text{SW}}$ and DIC change to reconstruct CO_2 climate forcing. In
692 the absence of detailed constraints on $\delta^{11}\text{B}_{\text{SW}}$ and a second carbonate system parameter
(e.g., DIC), we argue that only a sampling strategy that targets relatively abrupt
694 transitions or orbital cyclicity can yield robust quantification of pH change and the
associated CO_2 climate forcing. Furthermore, samples should be taken from low-latitude
696 open-ocean sites that are close to CO_2 equilibrium with the atmosphere, and exclude time
intervals with known biogeochemical aberrations (such as widespread anoxia or euxinia)

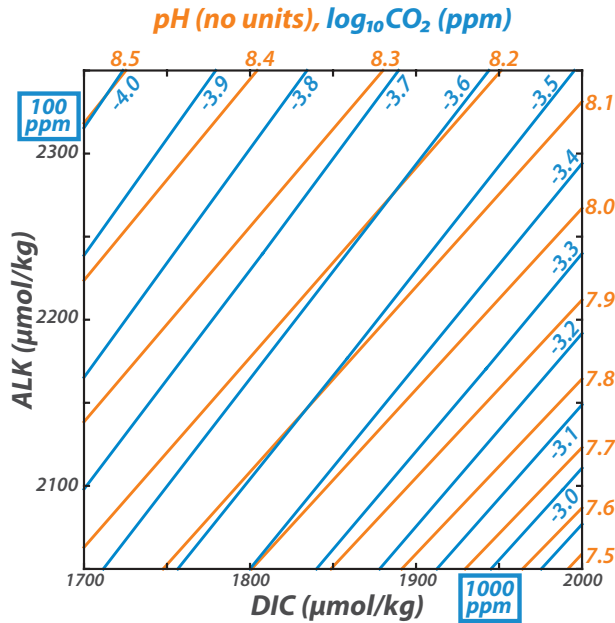
698 that may violate our formalism. With these caveats, we demonstrate that boron isotope
data can yield adequate constraints on CO₂ climate forcing.

700

Ultimately, we hope the formalism, theory and validation presented in this study opens
702 the door to utilize the boron isotope proxy system to derive quantitative constraints on the
various types of climate sensitivity (e.g. equilibrium and Earth system, ECS and ESS
704 respectively; cf. Lunt et al., 2010; PALEOSENS Project Members, 2012). Combined
with independent climate reconstructions and ice sheet modeling (e.g., PALEOSENS
706 Project Members, 2012; Köhler et al., 2015; Royer, 2016) these constraints will enable
the mapping out of changes in ESS and ECS (e.g., Köhler et al., 2015; von der Heydt et
708 al., 2016) as the planet transitioned from the early Cenozoic greenhouse to the recurring
Pleistocene ice ages, improving our understanding of our planet's climate machine as
710 well as honing projections of its future under continued anthropogenic perturbation.

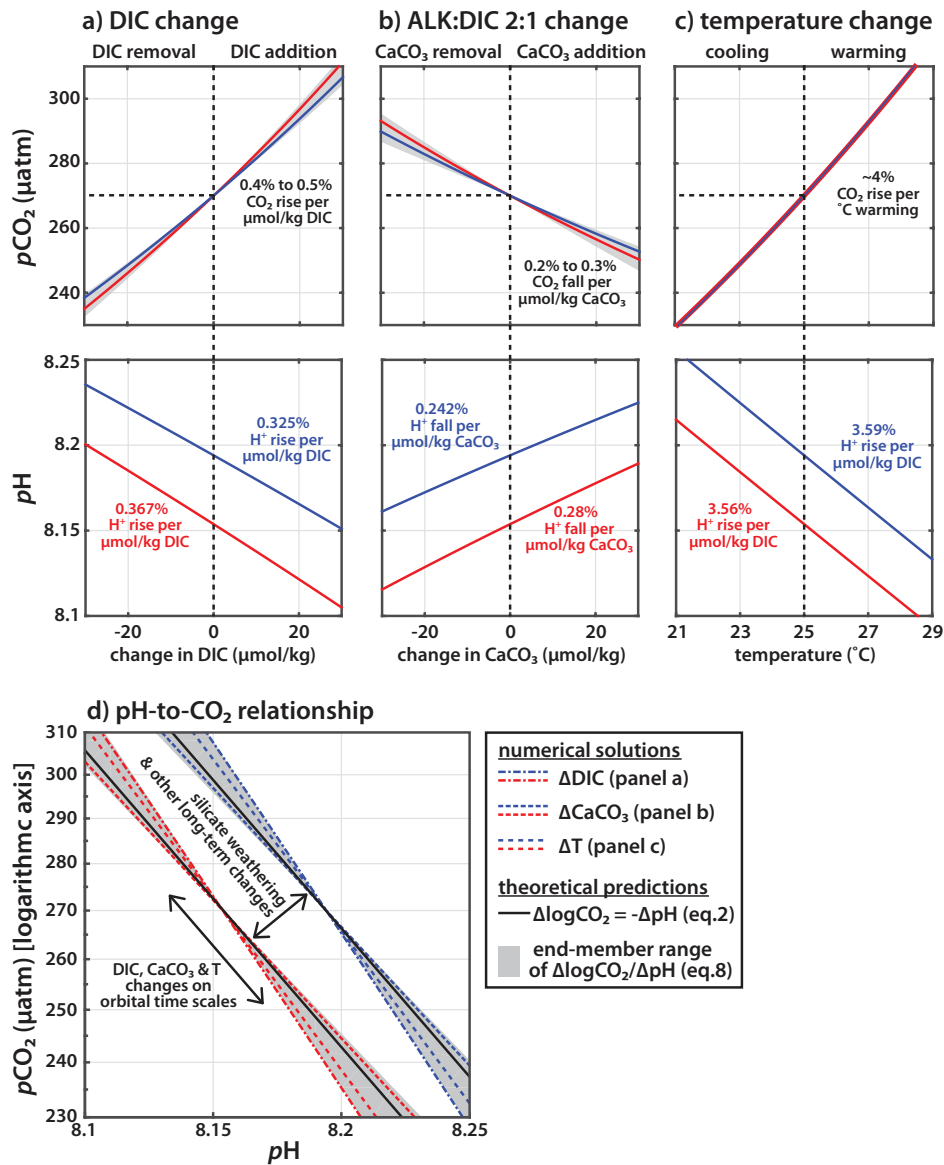
712 **Acknowledgement**

We thank Sarah Greene, an unnamed referee and the Associate Editor for helpful
714 comments and suggestions. This study was supported by UK Natural Environment
Research Council grants NE/K00901X/1 to MPH, NE/I006346/1 to GLF, NE/P011381/1
716 to GLF and MPH, and NE/I528626/1 to TC. The Pleistocene boron isotope data can be
found at <https://doi.pangaea.de/10.1594/PANGAEA.882551>.



718

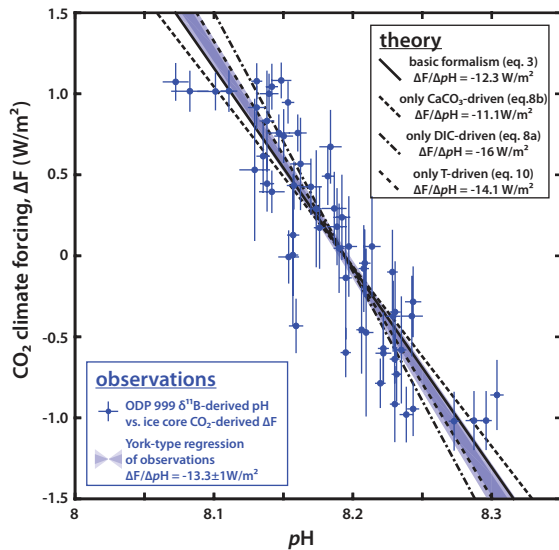
720 **Figure 1.** Illustration of the tight coupling between CO₂ and pH. Across a wide range of
722 dissolved inorganic carbon (DIC) and alkalinity (ALK) concentrations contours of
724 constant pH and constant CO₂ are broadly aligned, with similar spacing between pH and
726 log₁₀CO₂ contours. This suggests that H⁺ and CO₂ are approximately proportional across
the plotted field of DIC and ALK, which covers more than an order of magnitude CO₂
change. In this study we formally explore the mechanisms and implications of the pH-
CO₂ relationship in the context of our ability to reconstruct past CO₂ climate forcing.



728

Figure 2. Sensitivity of CO_2 partial pressure and pH to incremental perturbation of (a) DIC, (b) CaCO_3 with an alkalinity-to-DIC ratio of 2:1, (c) temperature, and (d) the relationships between CO_2 and pH of experiments (a) to (c). Blue and red lines indicate two separate experiments both with an initial CO_2 of 270 μatm but with initial DIC of 1800 $\mu\text{mol/kg}$ and 2000 $\mu\text{mol/kg}$, respectively. The black lines in (d) correspond to the pH- CO_2 relationship predicted from equation 2 (solid) and the numerical solutions as shown in panels (a) to (c) (dashed). The purpose of this figure is to demonstrate that fractional changes in CO_2 and H^+ are nearly equal (panels a, b and c), so as to yield ΔpH -to- $\Delta\log_{10}\text{CO}_2$ relationships close to -1-to-1 (panel d).

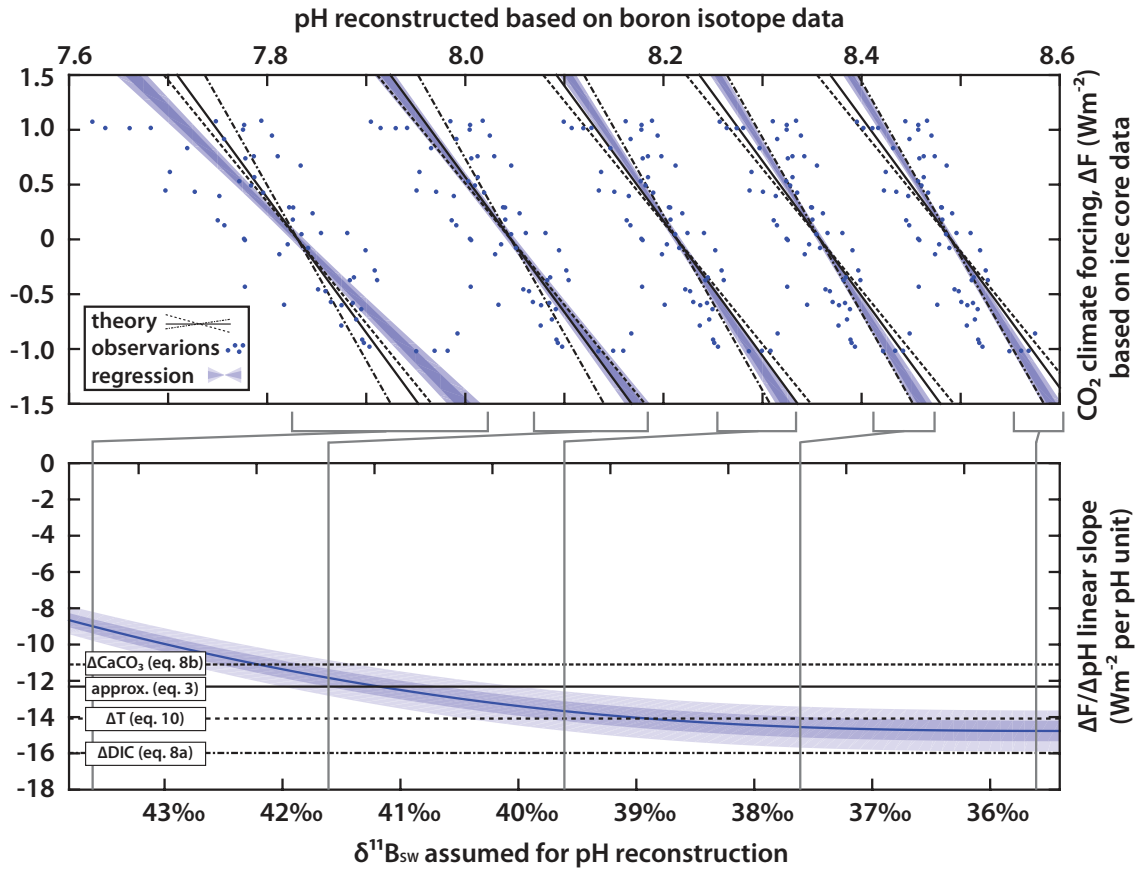
738



740

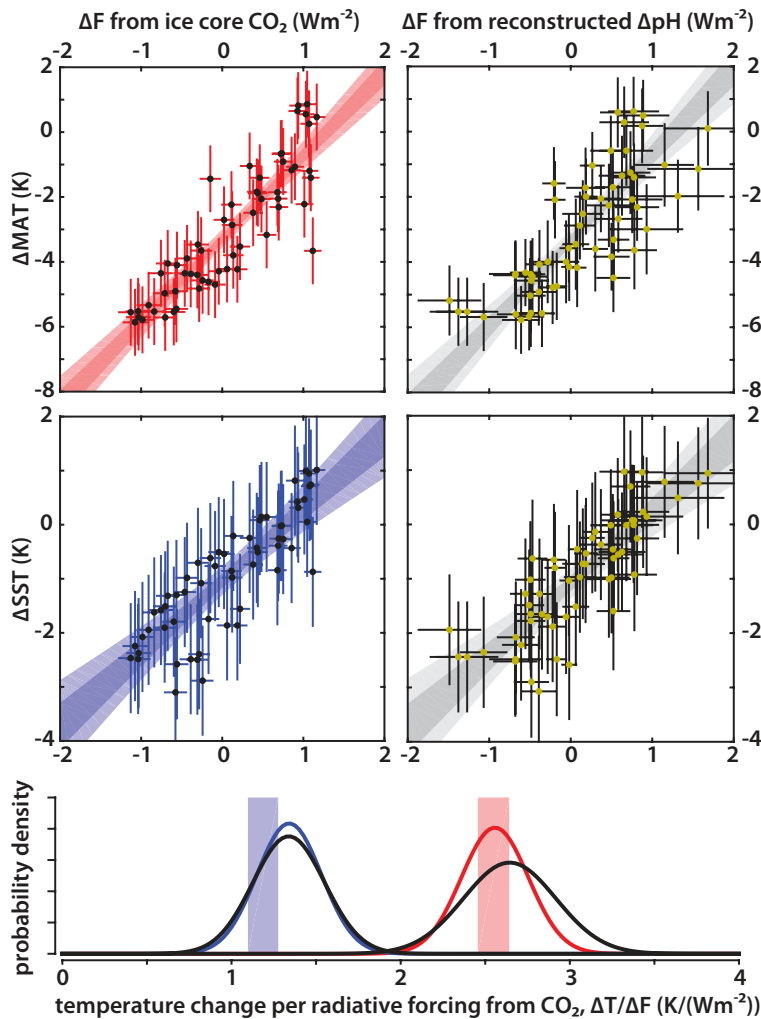
Figure 3. Relationship between CO₂ climate forcing from ice-core CO₂ reconstructions and pH from boron isotope record at ODP Site 999. The regression of the data is shown as blue shading, representing the 1σ and 2σ intervals confidence intervals. The regressed slope is statistically indistinguishable from that predicted by theory (equation 3), confirming a ΔpH-to-Δlog₁₀CO₂ relationship close to -1:1. The fact that the best-fit regressed slope is marginally lower than theory can be taken as evidence for the relative importance in driving glacial/interglacial CO₂ change of whole ocean alkalinity changes via the open system CaCO₃ cycle. This result is consistent with modeling results (Toggweiler, 1999; Hain et al., 2010).

750



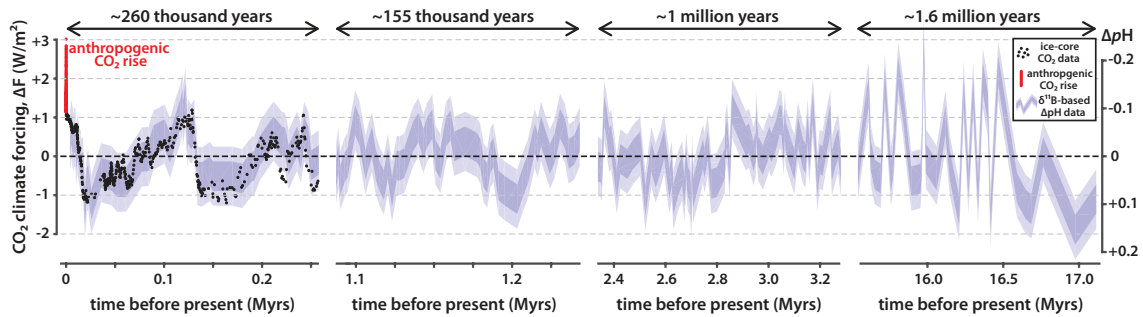
752 **Figure 4.** Relationship between ice core derived CO₂ climate forcing and ODP Site 999
 754 reconstructed pH, as in Figure 3 but this time ignoring reconstructed temperature and
 756 systematically introducing error in the seawater boron isotope composition ($\delta^{11}\text{B}_{\text{SW}}$)
 758 assumed in the pH reconstruction. The bottom panel compares observation regressed pH-
 CO₂ slope (blue shading) against theoretical prediction (solid and dashed black lines) as a
 function of systematically varied $\delta^{11}\text{B}_{\text{SW}}$. The top panel displays the observed, regressed
 and predicted pH-CO₂ relationship for five discrete cases: assuming true $\delta^{11}\text{B}_{\text{SW}}$ as well
 as deliberately introducing $\pm 2\text{‰}$ and $\pm 4\text{‰}$ error in $\delta^{11}\text{B}_{\text{SW}}$. This exercise demonstrates
 that reconstructed ΔpH is relatively insensitive to $\delta^{11}\text{B}_{\text{SW}}$ error, unlike absolute
 reconstructed pH.

762



764

Figure 5. Regression of climate sensitivity $\Delta T/\Delta F$ based on ice core CO_2 reconstructions
 766 (red and blue) and boron isotope data (black/gray), respectively. The four square panels
 768 (top) MAT and (bottom) SST (see Martinez-Boti et al., 2015), side by side for the two records of climate
 770 forcing (ice core left, and boron isotope right), whereby the ice core data was subsampled
 772 to the ages that are closest to the 59 boron isotope data points. The bottom panel shows
 774 the probability density functions for the regressed $\Delta T/\Delta F$ slope from the above panels,
 compared to the regressed slope for the all ice core CO_2 data of the last 260 kyrs
 (shading, 2σ). The standard error of ΔF determined from boron isotope data includes
 measurement uncertainty and the end member range of the ΔpH -to- ΔF conversion.



776

Figure 6. Reconstruction of CO₂ climate forcing using equations 3 and 6, based on
 778 Pleistocene, Plio-Pleistocene and mid-Miocene boron isotope records of Chalk et al.
 (2017), Martinez-Boti et al. (2013), and Greenop et al. (2014), respectively, with
 780 uncertainty envelope determined empirically from the offset to CO₂ climate forcing
 calculated from ice core data (black dots). This new approach for reconstructing CO₂
 782 climate forcing requires no assumption for a second carbon chemistry parameter and is
 relatively insensitive to error in $\delta^{11}\text{B}_{\text{sw}}$. Our formalism quantifies orbital-timescale CO₂
 784 climate forcing but not long-term changes such as between the different datasets or trends
 within the longer Plio-Pleistocene and Miocene datasets. That is, the conversion from
 786 ΔpH (right axis) to climate forcing (left axis) according to equation 3 is only valid for
 records that are shorter than the carbon residence time.

788

References

- 790 Bereiter, B., S. Eggleston, J. Schmitt, C. Nehrbass-Ahles, T. Stocker, H. Fischer, S.
792 Kipfstuhl, and J. Chappellaz (2015), Revision of the EPICA Dome C CO₂ record
from 800 to 600kyr before present, *Geophysical Research Letters*, 42(2), 542-549.
- Breecker, D., Z. Sharp, and L. McFadden (2010), Atmospheric CO₂ concentrations
794 during ancient greenhouse climates were similar to those predicted for AD 2100,
796 *Proceedings of the National Academy of Sciences of the United States of America*,
107(2), 576-580.
- Broecker, W. S., and T.-H. Peng (1987), The role of CaCO₃ compensation in the glacial
798 to interglacial atmospheric CO₂ change, *Global Biogeochemical Cycles*, 1(1), 15-29.
- Byrne, B., and C. Goldblatt (2014), Radiative forcing at high concentrations of well-
800 mixed greenhouse gases, *Geophysical Research Letters*, 41(1), 152-160.
- Chalk, T. B., et al. (2017), Causes of ice age intensification across the Mid-Pleistocene
802 Transition, *Proceedings of the National Academy of Sciences of the United States of
America*, 114(50), 13114-13119.
- 804 Foster, G. (2008), Seawater pH, PCO₂ and [CO₃²⁻] variations in the Caribbean Sea over
the last 130 kyr: A boron isotope and B/Ca study of planktic foraminifera, *Earth and
806 Planetary Science Letters*, 271(1-4), 254-266.
- Foster, G., P. Pogge von Strandmann, and J. Rae (2010), Boron and magnesium isotopic
808 composition of seawater, *Geochemistry Geophysics Geosystems*, 11.
- Foster, G., C. Lear, and J. Rae (2012), The evolution of pCO₂, ice volume and climate
810 during the middle Miocene, *Earth and Planetary Science Letters*, 341, 243-254.
- Foster, G. L., and J. W. B. Rae (2016), Reconstructing Ocean pH with Boron Isotopes in
812 Foraminifera, *Annual Review of Earth and Planetary Sciences*, Vol 44, 44, 207-237.
- Foster, G., J. Rae, R. Jeanloz, and K. Freeman (2016), Reconstructing Ocean pH with
814 Boron Isotopes in Foraminifera, *Annual Review of Earth and Planetary Sciences*, Vol
44, 44, 207-237.
- 816 Foster, G., B. Honisch, G. Paris, G. Dwyer, J. Rae, T. Elliott, J. Gaillardet, N. Hemming,
818 P. Louvat, and A. Vengosh (2013), Interlaboratory comparison of boron isotope
analyses of boric acid, seawater and marine CaCO₃ by MC-ICPMS and NTIMS,
Chemical Geology, 358, 1-14.
- 820 Franks, P., D. Royer, D. Beerling, P. Van de Water, D. Cantrill, M. Barbour, and J. Berry
(2014), New constraints on atmospheric CO₂ concentration for the Phanerozoic,
822 *Geophysical Research Letters*, 41(13), 4685-4694.
- Goodwin, P., A. Katavouta, V. M. Roussenov, G. L. Foster, E. J. Rohling, and R. G.
824 Williams (2018), Pathways to 1.5 degrees C and 2 degrees C warming based on
observational and geological constraints, *Nature Geoscience*, 11(2), 102-+.
- 826 Greenop, R., G. Foster, P. Wilson, and C. Lear (2014), Middle Miocene climate
instability associated with high-amplitude CO₂ variability, *Paleoceanography*, 29(9),
828 845-853.

- 830 Greenop, R., M. Hain, S. Sosdian, K. Oliver, P. Goodwin, T. Chalk, C. Lear, P. Wilson,
and G. Foster (2017), A record of Neogene seawater delta B-11 reconstructed from
832 paired delta B-11 analyses on benthic and planktic foraminifera, *Climate of the Past*,
13(2), 149-170.
- 834 Hain, M., D. Sigman, and G. Haug (2010), Carbon dioxide effects of Antarctic
stratification, North Atlantic Intermediate Water formation, and subantarctic nutrient
836 drawdown during the last ice age: Diagnosis and synthesis in a geochemical box
model, *Global Biogeochemical Cycles*, 24.
- 838 Hain, M., D. Sigman, J. Higgins, and G. Haug (2015), The effects of secular calcium and
magnesium concentration changes on the thermodynamics of seawater acid/base
840 chemistry: Implications for Eocene and Cretaceous ocean carbon chemistry and
buffering, *Global Biogeochemical Cycles*, 29(5), 517-533.
- 842 Hain, M. P., D. M. Sigman, and G. H. Haug (2014), The Biological Pump in the Past,
Treatise on Geochemistry 2nd edition, 485-517.
- 844 Hemming, N., and G. Hanson (1992), Boron isotopic composition and concentration in
modern marine carbonates, *Geochimica Et Cosmochimica Acta*, 56(1), 537-543.
- 846 Hemming, N. G., and B. Hönisch (2007), Boron Isotopes in Marine Carbonate Sediments
and the pH of the Ocean in *Developments in Marine Geology*, pp. 717-734.
- 848 Henehan, M., P. Hull, D. Penman, J. Rae, and D. Schmidt (2016), Biogeochemical
significance of pelagic ecosystem function: an end-Cretaceous case study,
Philosophical Transactions of the Royal Society B-Biological Sciences, 371(1694).
- 850 IPCC (2014): Climate Change 2014: Synthesis Report. Contribution of Working Groups
I, II and III to the Fifth Assessment Report of the Intergovernmental Panel on Climate
852 Change [Core Writing Team, R.K. Pachauri and L.A. Meyer (eds.)]. IPCC, Geneva,
Switzerland, 151 pp.
- 854 Klochko, K., A. J. Kaufman, W. Yao, R. H. Byrne, and J. A. Tossell (2006),
Experimental measurement of boron isotope fractionation in seawater, *Earth and*
856 *Planetary Science Letters*, 248(1-2), 276-285.
- 858 Knutti, R., and G. C. Hegerl (2008), The equilibrium sensitivity of the Earth's temperature to
radiation changes, *Nature Geoscience*, 1(11), 735-743.
- 860 Knutti, R., M. A. A. Rugenstein, and G. C. Hegerl (2017), Beyond equilibrium climate
sensitivity, *Nature Geoscience*, 10(10), 727-+.
- 862 Köhler, P., B. de Boer, A. von der Heydt, L. Stap, and R. van de Wal (2015), On the state
dependency of the equilibrium climate sensitivity during the last 5 million years,
Climate of the Past, 11(12), 1801-1823.
- 864 Lemarchand, D., J. Gaillardet, E. Lewin, and C. Allegre (2000), The influence of rivers
on marine boron isotopes and implications for reconstructing past ocean pH, *Nature*,
866 408(6815), 951-954.
- 868 Lemarchand, D., J. Gaillardet, E. Lewin, and C. Allegre (2002), Boron isotope
systematics in large rivers: implications for the marine boron budget and paleo-pH
reconstruction over the Cenozoic, *Chemical Geology*, 190(1-4), 123-140.

- 870 Lunt, D., A. Haywood, G. Schmidt, U. Salzmann, P. Valdes, and H. Dowsett (2010),
Earth system sensitivity inferred from Pliocene modelling and data, *Nature*
872 *Geoscience*, 3(1), 60-64.
- Martinez-Boti, M., G. Foster, T. Chalk, E. Rohling, P. Sexton, D. Lunt, R. Pancost, M.
874 Badger, and D. Schmidt (2015), Plio-Pleistocene climate sensitivity evaluated using
high-resolution CO₂ records, *Nature*, 518(7537), 49-+.
- 876 Martinez-Garcia, A., D. Sigman, H. Ren, R. Anderson, M. Straub, D. Hodell, S. Jaccard,
T. Eglinton, and G. Haug (2014), Iron Fertilization of the Subantarctic Ocean During
878 the Last Ice Age, *Science*, 343(6177), 1347-1350.
- Myhre, G., E. Highwood, K. Shine, and F. Stordal (1998), New estimates of radiative
880 forcing due to well mixed greenhouse gases, *Geophysical Research Letters*, 25(14),
2715-2718.
- 882 Pagani, M. (2014), Biomarker-Based Inferences of Past Climate: The
Alkenone pCO₂ Proxy, *Treatise on Geochemistry* 2nd edition, pp. 361-378.
- 884 Pagani, M., D. Lemarchand, A. Spivack, and J. Gaillardet (2005), A critical evaluation of
the boron isotope-pH proxy: The accuracy of ancient ocean pH estimates,
886 *Geochimica Et Cosmochimica Acta*, 69(4), 953-961.
- PALEOSENS Project Members (2012), Making sense of palaeoclimate sensitivity,
888 *Nature*, 491(7426), 683-691.
- Pearson, P., and M. Palmer (2000), Atmospheric carbon dioxide concentrations over the
890 past 60 million years, *Nature*, 406(6797), 695-699.
- Rae, J., G. Foster, D. Schmidt, and T. Elliott (2011), Boron isotopes and B/Ca in benthic
892 foraminifera: Proxies for the deep ocean carbonate system, *Earth and Planetary*
Science Letters, 302(3-4), 403-413.
- 894 Raitzsch, M., and B. Hönisch (2013), Cenozoic boron isotope variations in benthic
foraminifers, *Geology*, 41(5), 591-594.
- 896 Rodenbeck, C., R. Keeling, D. Bakker, N. Metz, A. Olsen, C. Sabine, and M. Heimann
(2013), Global surface-ocean p(CO₂) and sea-air CO₂ flux variability from an
898 observation-driven ocean mixed-layer scheme, *Ocean Science*, 9(2), 193-216.
- Rohling, E. J., G. Marino, G. L. Foster, P. A. Goodwin, A. S. von der Heydt, and P.
900 Koehler (2018), Comparing Climate Sensitivity, Past and Present, *Annual Review of*
Marine Sciences, Vol 10, 10, 261-+.
- 902 Royer, D. (2006), CO₂-forced climate thresholds during the Phanerozoic, *Geochimica Et*
Cosmochimica Acta, 70(23), 5665-5675.
- 904 Royer, D., R. Jeanloz, and K. Freeman (2016), Climate Sensitivity in the Geologic Past,
Annual Review of Earth and Planetary Sciences, Vol 44, 44, 277-293.
- 906 Shakun, J. D., P. U. Clark, F. He, S. A. Marcott, A. C. Mix, Z. Liu, B. Otto-Bliesner, A.
Schmittner, and E. Bard (2012), Global warming preceded by increasing carbon
908 dioxide concentrations during the last deglaciation, *Nature*, 484(7392), 49-54.
- Sigman, D., and E. Boyle (2000), Glacial/interglacial variations in atmospheric carbon

- 910 dioxide, *Nature*, 407(6806), 859-869.
- 912 Sigman, D., M. Hain, and G. Haug (2010), The polar ocean and glacial cycles in atmospheric CO₂ concentration, *Nature*, 466(7302), 47-55.
- 914 Spivack, A., and J. Edmond (1987), Boron isotope exchange between seawater and the oceanic-crust, *Geochimica Et Cosmochimica Acta*, 51(5), 1033-1043.
- 916 Spivack, A., C. You, and H. Smith (1993), Foraminiferal Boron isotope ratios as a proxy for surface ocean pH over the past 21-Myr, *Nature*, 363(6425), 149-151.
- 918 Takahashi, T., et al. (2002), Global sea-air CO₂ flux based on climatological surface ocean pCO₂, and seasonal biological and temperature effects, *Deep-Sea Research Part II-Topical Studies in Oceanography*, 49(9-10), 1601-1622.
- 920 Takahashi, T., et al. (2009), Climatological mean and decadal change in surface ocean pCO₂, and net sea-air CO₂ flux over the global oceans, *Deep-Sea Research Part II-Topical Studies in Oceanography*, 56(8-10), 554-577.
- 922
- 924 Vengosh, A., Y. Kolodny, A. Starinsky, A. Chivas, and M. McCulloch (1991), Coprecipitation and isotopic fractionation of Boron in modern biogenic carbonates, *Geochimica Et Cosmochimica Acta*, 55(10), 2901-2910.
- 926 van de Wal, R. S. W., B. de Boer, L. J. Lourens, P. Koehler, and R. Bintanja (2011), Reconstruction of a continuous high-resolution CO₂ record over the past 20 million years, *Climate of the Past*, 7(4), 1459-1469.
- 928
- 930 von der Heydt, A.S., et al. (2016) Lessons on Climate Sensitivity From Past Climate Changes, *Current Climate Change Reports*, 2, 148-158, doi:10.1007/s40641-016-0049-3
- 932 Wang, X., et al. (2017), Deep-sea coral evidence for lower Southern Ocean surface nitrate concentrations during the last ice age, *Proceedings of the National Academy of Sciences of the United States of America*, 114(13), 3352-3357.
- 934
- 936 York, D., N. M. Evensen, M. L. Martinez, and J. D. Delgado (2004), Unified equations for the slope, intercept, and standard errors of the best straight line, *American Journal of Physics*, 72(3), 367-375.
- 938 Zachos, J. C., G. R. Dickens, and R. E. Zeebe (2008), An early Cenozoic perspective on greenhouse warming and carbon-cycle dynamics, *Nature*, 451(7176), 279-283.
- 940 Zeebe, R. E., and D. Wolf-Gladrow (2001), Stable Isotope Fractionation, in *CO₂ in Seawater: Equilibrium, Kinetics, Isotopes*, pp. 141-250, Elsevier.